CI-CBM: Class-Incremental Concept Bottleneck Model for Interpretable Continual Learning

Anonymous authors
Paper under double-blind review

Abstract

Catastrophic forgetting remains a fundamental challenge in continual learning, in which models often forget previous knowledge when fine-tuned on a new task. This issue is especially pronounced in class incremental learning (CIL), which is the most challenging setting in continual learning. Existing methods to address catastrophic forgetting often sacrifice either model interpretability or accuracy. To address this challenge, we introduce Class-Incremental Concept Bottleneck Model (**CI-CBM**), which leverage novel techniques, including concept regularization and pseudo-concept generation to maintain interpretable decision processes throughout incremental learning phases. Through extensive evaluation on seven benchmark datasets, **CI-CBM** achieves comparable performance to black-box models and significantly outperforms previous interpretable approaches in CIL, with an average 36% accuracy gain. **CI-CBM** provides both interpretable decisions on individual inputs and understandable global decision rules, as shown in our experiments, thereby demonstrating that human-understandable concepts can be maintained during incremental learning without compromising model performance. Our approach is effective in both pretrained and non-pretrained scenarios; in the latter, the backbone is trained from scratch during the first learning phase.

1 Introduction

Deep learning models have demonstrated exceptional performance when trained on large-scale, stationary datasets all at once, as evidenced by breakthroughs in computer vision (He et al., 2016), healthcare (Ronneberger et al., 2015; Zhang et al., 2024), robotics (Mnih, 2013), and autonomous driving (Bojarski, 2016). However, their performance deteriorates substantially when data arrives sequentially over time (De Lange et al., 2021). Continuously retraining models from scratch each time new data arrives is computationally expensive, time-consuming, and impractical. These limitations have spurred growing interest in continual learning, a different learning paradigm that seeks to enable models to learn from evolving data streams efficiently without forgetting previously acquired knowledge.

Continual learning (Parisi et al., 2019) enables models to incrementally update their knowledge and adapt to new data over time. In this work, we focus on the class incremental learning (CIL) setting (Van de Ven & Tolias, 2019), which is widely regarded as the most challenging form of continual learning. In CIL, each phase introduces a new set of classes disjoint from previously seen ones, and at inference time, a single model must classify test samples from all observed classes without access to phase identifiers. A central difficulty in this setting is *catastrophic forgetting* (McCloskey & Cohen, 1989; Goodfellow et al., 2013), where learning new tasks often interferes with previously acquired knowledge, leading to substantial accuracy degradation on earlier tasks.

To address catastrophic forgetting in CIL, conventional methods utilize a bounded buffer to store a subset of exemplars (Rebuffi et al., 2017; Hou et al., 2019; Wu et al., 2019) from previous phases. The model is then fine-tuned jointly on both the current phase data and the stored data. However, this approach raises concerns regarding privacy and storage limitations. Recently, the Exemplar-Free CIL (EFCIL) approach has gained increasing attention (Zhu et al., 2021b; 2022; Petit et al., 2023). The main challenge in this approach

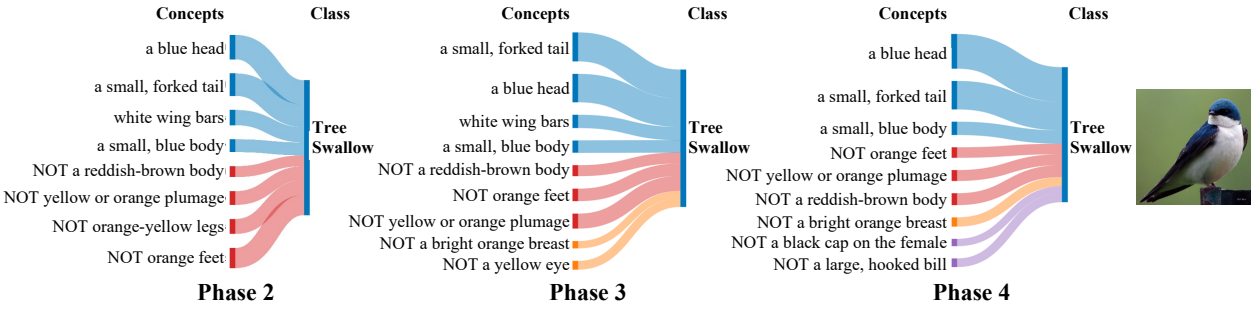

Figure 1: Visualization of the final layer weights with absolute values greater than 0.2 for the **Tree Swallow** class in the CUB dataset under a four-phase scenario. Concepts with negative weights are labeled as "NOT" concepts. Positive and negative concepts in phase 2 are shown in blue and red, respectively, while concepts added in phases 3 and 4 are shown in orange and purple. As new phases arrive, CI-CBM can preserve the positive concepts while learning more discriminative negative features. The thickness of each edge corresponds to the absolute value of the weight. Additional visualizations are provided in Supplement Section A12.

is to classify between old and new classes without access to old data. Some approaches (Zhu et al., 2021b; 2022) propose fine-tuning the model on new classes while employing knowledge distillation (Hinton, 2015) to preserve the learned knowledge from old classes. Others (Belouadah & Popescu, 2018; Petit et al., 2023; Panos et al., 2023) freeze the feature extractor after the first phase and focus on incrementally learning the classifier in the next phases. Meanwhile, other methods (Wang et al., 2022c;b; Smith et al., 2023) employ a backbone model that has been pretrained on large-scale datasets. However, these models depend heavily on strong pretraining and exhibit a significant performance drop when the backbone is trained on first-phase data instead of a large-scale dataset (Tang et al., 2023).

Although recent advancements in CIL offer promising solutions to catastrophic forgetting, the decision-making mechanisms of these models are often difficult to understand and are regarded as *black-box* processes. Interpretability is crucial for uncovering the information a model uses when classifying inputs, which is critical for identifying biases and debugging. Recently, researchers have developed methods to interpret black-box deep neural networks (DNNs) in continual learning (Patra & Noble, 2020; Guzy et al., 2021). However, most methods focus on examining the DNN model after training is complete, with only a few approaches, such as ICICLE (Rymarczyk et al., 2023) and IN2 (Yang et al., 2024), focusing on learning models that are interpretable by design. Despite being pioneering work in this direction, ICICLE is restricted to specific architectures and fine-grained datasets, while IN2's suboptimal concept expansion compromises efficiency. Moreover, the performance gap between current interpretable models and unrestricted ones in CIL further diminishes the incentive to adopt interpretable approaches, as their reduced accuracy makes the models less practical for real-world use. These limitations motivate our work to develop a more generalizable and inherently interpretable approach to class incremental learning, suitable for both pretrained and non-pretrained model scenarios.

In this paper, we propose a new framework called the Class Incremental Concept Bottleneck Model (**CI-CBM**) to extend the Concept Bottleneck Model (CBM) for the challenging Exemplar-Free CIL (EFCIL) setting. In the EFCIL setting, due to the absence of samples from previous classes, the learned functionality of each concept and its contribution to those classes must be preserved while allowing the model to continually learn new concepts and adjust their contributions across all classes. To address these problems, **CI-CBM** employs an effective mechanism to prevent concept drift and mitigate classifier bias (see Figure 1 and 6). Our contributions are summarized below:

- We introduce a new approach to learn inherently interpretable neural models for class incremental learning with much better performance and utility. Unlike previous interpretable approaches in CIL, our approach **CI-CBM** achieves 25–43% higher accuracy across multiple benchmarks while

maintaining scalability and adaptability across various datasets and architectures, demonstrating strong performance both with pretrained backbone models and when trained from scratch.

- We propose new techniques including concept regularization to prevent the learned concepts from losing their functionality while learning new concepts. Additionally, we utilize pseudo-concepts for previous class data in conjunction with actual concepts for new class data to incrementally train the sparse classifier across different phases.
- We evaluate our approach by conducting comprehensive EFCIL evaluation scenarios and performing ablation studies to assess the impact of different components of the proposed method. The results demonstrate the superiority of our method over other interpretable models in CIL, achieving an average accuracy gain of 36%.

2 Related work

2.1 Class Incremental Learning

Class Incremental Learning (CIL) aims to extend the capabilities of deep learning models to continuously learn from new data and adapt to new classes over time while retaining previously acquired knowledge. The goal is to develop a model that can classify all previously seen classes effectively at any stage of training, which requires a balance between plasticity—the flexibility to learn new features—and stability—the resistance to forgetting old information. The phenomenon of catastrophic forgetting (McCloskey & Cohen, 1989; Goodfellow et al., 2013) illustrates a fundamental trade-off in CIL, where the effort to incorporate new information can result in the loss of valuable knowledge from previous phases, leading to a sharp drop in performance on previous classes.

To address catastrophic forgetting, several approaches have been proposed: **(I)** Regularization-based methods: These approaches (Kirkpatrick et al., 2017; Aljundi et al., 2018; Wang et al., 2021) mitigate forgetting by constraining changes in critical parameters across phases. However, these methods lack reliable metrics for parameter importance and perform poorly in CIL (Van de Ven & Tolias, 2019). **(II)** Architecture-based methods: These approaches expand network capacity dynamically when a new phase arrives (Rusu et al., 2016; Yan et al., 2021; Yoon et al., 2017). However, a key challenge is the increasing memory and computational costs as the architecture grows, making it crucial to manage the rate of expansion with each phase. **(III)** Rehearsal-based methods: These approaches utilize various sampling strategies, such as herding (Rebuffi et al., 2017), diversity-aware sampling (Bang et al., 2021), reservoir sampling (Buzzega et al., 2020), and greedy sampling (Prabhu et al., 2020), to store samples in bounded memory. These samples are then used for knowledge distillation (Li & Hoiem, 2017; Rebuffi et al., 2017; Dhar et al., 2019; Douillard et al., 2020), bias correction (Hou et al., 2019; Wu et al., 2019), or gradient regularization (Lopez-Paz & Ranzato, 2017; Chaudhry et al., 2018). Despite their effectiveness in addressing catastrophic forgetting, rehearsal-based methods pose privacy risks, as storing data from previous phases may expose confidential information, particularly in sensitive areas like healthcare. Generative models can be trained to produce samples from previous classes (Wu et al., 2018; Gao & Liu, 2023), but they are prone to catastrophic forgetting (Thanh-Tung & Tran, 2020) and are vulnerable to model-inversion attacks (Zhang et al., 2020), which may leak personal data.

Recently, Exemplar-Free Class Incremental Learning (EFCIL) approaches have gained popularity. These methods often focus on learning high-quality feature representations in the first phase, which usually covers around half of the total classes. For instance, FeTrIL (Petit et al., 2023) freezes the feature extractor after this initial phase and generates pseudo-features using basic geometric transformations based on the class mean. The aim of such methods is to maximize the utility of the representations learned in the first phase for the subsequent phases.

Recent advancements have introduced methods that leverage ImageNet-pretrained ViT models. Among these, some approaches (Wang et al., 2022c;b;a; Smith et al., 2023; Tang et al., 2023) introduce lightweight prompts that are concatenated with input patches and processed alongside them, enabling task-specific adaptation without modifying backbone weights. These methods maintain a pool of prompts, selecting

or generating instance-specific ones through key-query matching (Wang et al., 2022c), clustering (Wang et al., 2022a), or attention-based combinations (Smith et al., 2023). However, these methods require a strong pretrained backbone and tend to experience performance degradation when the data from the first phase is used for pretraining the backbone (Tang et al., 2023). In addition, the core idea of CIL is to enable a system to acquire knowledge that was previously unavailable (Zhou et al., 2024b). The use of large pretraining datasets like ImageNet raises the question of whether these models encounter truly novel information. However, our approach reduces dependence on extensive pretraining, making it applicable to both pretrained and non-pretrained scenarios.

2.2 Interpretability

Despite advancements in CIL methods, there remains a gap in understanding how these black-box models function. Interpretability frameworks aim to make the decision-making process of models more transparent. Rather than relying on post-hoc explanations for black-box models, it is more effective to design models that are inherently interpretable, reducing the risk of misleading interpretations and potential harm in high-stakes applications (Rudin, 2019).

The Concept Bottleneck Model (CBM) (Koh et al., 2020) incorporates an intermediate concept bottleneck layer, where each neuron corresponds to a human-understandable concept. This allows the model's final prediction to be expressed as a linear combination of interpretable concepts, significantly improving our insight into how decisions are made. CBM requires dense concept annotations in the training data to learn the bottleneck layer, limiting its scalability and applicability. LF-CBM (Oikarinen et al., 2023) addresses this issue by automating the CBM training process, thus reducing reliance on human experts. LF-CBM leverages Large Language Models, such as GPT-3, to gather relevant concepts for each task and aligns image-concept activations using vision-language models like CLIP (Radford et al., 2021) and the neuron-level interpretability tool CLIP-Dissect (Oikarinen & Weng, 2023). CBMs have demonstrated significant potential across domains, including medical applications (Yuksekgonul et al., 2022), deep generative models (Ismail et al., 2023; Kulkarni et al., 2025), and large language models (Sun et al., 2025).

Although interpretability is well-established in classical machine learning, it remains underexplored in the context of continual learning. ICICLE (Rymarczyk et al., 2023) introduced interpretability in class incremental learning through prototypical parts. However, their work is limited to specific model architectures and fine-grained datasets. Recently, IN2 (Yang et al., 2024) extended the CBM by freezing learned concepts and regularizing the prediction layer. However, the expansion of the concept set in their approach is not optimal, and its performance is much weaker than that of unrestricted models.

Generally, there is a trade-off between interpretability and accuracy. Previous works, such as PCBM (Yuksekgonul et al., 2022) (e.g., their Tables 1 and 2) demonstrate that interpretable models generally suffer from lower accuracy compared to their black-box counterparts in classical machine learning. LF-CBM (Oikarinen et al., 2023) (e.g., their Table 2) alleviates this trade-off by improving accuracy in standard image classification tasks. However, we found that the gap is more pronounced in the context of CIL. As the performance gap between interpretable and unrestricted models widens, the motivation to use interpretable models diminishes. In contrast, our proposed method bridges this gap by providing interpretability with minimal accuracy gap.

3 Methods

To make this work self-contained, we begin by reviewing the Label-free Concept Bottleneck Models (LF-CBM) framework and then explain how we adapt it for the EFCIL scenario.

3.1 Label-free Concept Bottleneck Models (LF-CBM)

Concept Set Creation and Filtering. The concept set refers to the group of concepts included in the interpretable concept bottleneck layer. These concepts represent features that are both important to the problem and easy for humans to understand, such as key features, common surrounding items, and

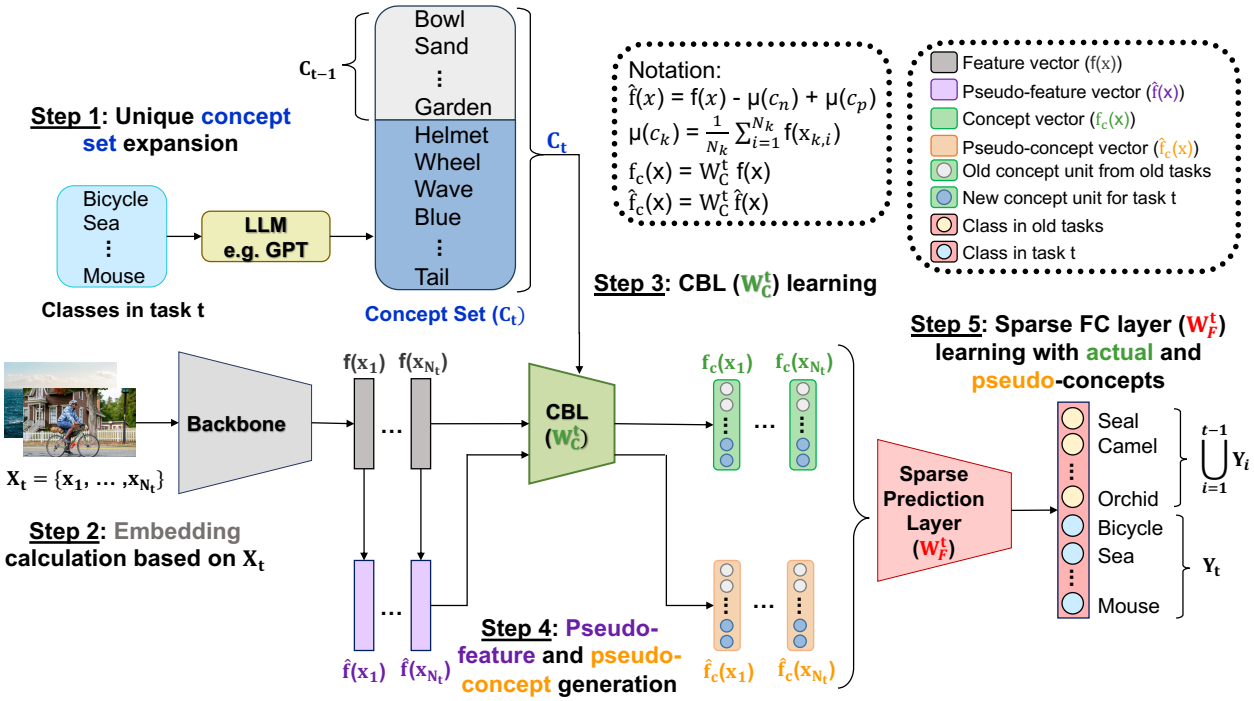

Figure 2: Overview of our pipeline for Class Incremental Concept Bottleneck Model (CI-CBM). Color-coded text matches the corresponding stages in the figure.

superclasses. These concepts are generated automatically by prompting GPT-3 to identify concepts related to each class in the dataset. The concepts for all classes are then combined to form an initial concept set. This set is further refined by filtering out concepts that are too lengthy, those that closely resemble the class names, and concepts that are similar to each other.

Learning the Concept Bottleneck Layer. The next step involves learning the projection weights W_C, which map the frozen backbone model's feature space onto a space where the axes correspond to interpretable concepts. Let $C = \{t_1, \dots, t_M\}$ represent the concept set, and $D = \{x_1, \dots, x_N\}$ the training dataset. The concept activation matrix P is calculated and stored, where $P_{i,j} = E_I(x_i) \cdot E_T(t_j)$, with E_I and E_T denoting the CLIP image and text encoders, respectively. The weights W_C are optimized to maximize the similarity between the neuron's activation patterns and the target concepts. The similarity is measured using the differentiable *Cos cubed* function, defined as:

$$L(W_C) = \sum_{i=1}^{M} -\text{sim}(t_i, q_i) := \sum_{i=1}^{M} -\frac{\bar{q}_i^3 \cdot \bar{P}_{:,i}^3}{\|\bar{q}_i^3\|_2 \|\bar{P}_{:,i}^3\|_2} \tag{1}$$

Here, q_i denotes the activation of the i-th neuron in the projection layer, and $\bar{q}$ represents q normalized to have mean 0 and standard deviation 1.

Learning the Sparse Final Layer. The final step involves learning a sparse predictor, W_F, using the GLM-SAGA (Wong et al., 2021) solver with an elastic net objective.

$$\min_{W_F, b_F} \sum_{i=1}^{N} L_{ce}(W_F f_c(x_i) + b_F, y_i) + \lambda R_\alpha(W_F) \tag{2}$$

where $R_\alpha(W_F) = (1-\alpha)\frac{1}{2}\|W_F\|_F + \alpha\|W_F\|_{1,1}$, with $\|\cdot\|_F$ representing the Frobenius norm and $\|\cdot\|_{1,1}$ the element-wise matrix norm, and $f_c(x) = W_C f(x)$ denotes the projection of backbone features into the concept space.

3.2 Class Incremental Concept Bottleneck Model (CI-CBM)

To adapt LF-CBM for the class incremental learning setting, we introduce three main modules, as illustrated in Figure 2: (I) curated concept set expansion (Step 1), (II) knowledge-preserving concept learning (Step 2-3), and (III) dynamic adaptation in the sparse prediction layer (Step 4-5). Let $D = \{D_1, D_2, \ldots, D_T\}$ denote the sequence of datasets from the first to the last phase T, where each dataset $D_t = \{X_t, Y_t\} = \{x_{t,j}, y_{t,j}\}_{j=1}^{N_t}$ consists of N_t labeled samples received by the model at phase t. The classes across different phases are disjoint, and the phase boundaries remain unknown during testing. When the first batch of data, D_1, arrives, the model is trained following the LF-CBM approach, as outlined in Section 3.1. After completing the learning process for phase $t-1$, the model has a concept set C_{t-1}, containing M_{t-1} concepts related to the previously seen classes ($\bigcup_{i=1}^{t-1} Y_i$), along with a concept bottleneck layer W_C^{t-1} and a unified sparse prediction layer W_F^{t-1}.

Module (I): Incremental Concept Set Expansion. When a new phase t begins, concepts for the new classes are generated using GPT-3, filtered, and added to the concept set. If concepts related to the new classes already exist due to their similarity to previous classes, they are not added again. As a result, the updated concept set C_t contains M_t unique concepts. Next, the concept activation matrix $P^t \in \mathbb{R}^{N_t \times M_t}$ is computed using a multimodal model based on the new training dataset D_t and the combined concept set C_t. In our experiments, we used SigLIP (Zhai et al., 2023) instead of CLIP (Radford et al., 2021), which is used in LF-CBM (Oikarinen et al., 2023), as the multimodal model for computing P^t. SigLIP is a recent model that focuses on image-text pairs and employs a sigmoid loss function, in contrast to the softmax-based contrastive learning approach used in CLIP.

Module (II): Preventing Concept Drift in the Concept Bottleneck Layer with Distillation Loss. As the concept set expands, the learned W_C^{t-1} is adjusted to accommodate new neurons for the added concepts, resulting in W_C^t, which must be learned. Naively fine-tuning W_C^t on D_t risks shifting the functionality of previously learned concepts to the new data, leading to catastrophic forgetting of past knowledge. Conversely, freezing the learned concepts to prevent updates limits the model's adaptability. Before expanding W_C^{t-1} to accommodate new concepts, the scores for the current concepts on the dataset from the new phase are calculated and saved. During the training of the concept bottleneck layer, an additional distillation loss is introduced to regularize the loss function, aiming to prevent the output of the current model (W_C^t) from drifting too far from the saved output of the previous model (W_C^{t-1}). The loss function for learning W_C^t is defined as:

$$L(W_C^t) = \sum_{i=1}^{M_t} -\frac{\bar{q}_i^{t\,3} \cdot \bar{P}_{:,i}^{t\,3}}{\|\bar{q}_i^{t\,3}\|_2 \|\bar{P}_{:,i}^{t\,3}\|_2} + \sum_{i=1}^{M_{t-1}} -\frac{\bar{q}_i^{t\,3} \cdot \bar{q}_i^{t-1\,3}}{\|\bar{q}_i^{t\,3}\|_2 \|\bar{q}_i^{t-1\,3}\|_2} \tag{3}$$

Module (III): Dynamic Adaptation of Prediction Layer and Pseudo-Concept Generation. The prediction layer, W_F^t, and its bias, b_F^t, must be expanded to accommodate both new concepts and class labels, while preserving the learned associations between previous classes and concepts stored in W_F^{t-1} and b_F^{t-1}. Following (Petit et al., 2023), we generate pseudo-features for past classes by shifting the data distribution of the nearest new class from the new class mean to the target past class mean, as shown in Figure 3. The centroids of each class in the backbone's feature space are computed and stored as the class is introduced. For each past class, its nearest new class is identified by calculating the cosine similarity between their centroids. Let c_p denote each past class, c_n the closest new class to c_p, and $\mu(c_p)$ and $\mu(c_n)$ the mean features of classes c_p and c_n, respectively, as extracted by the frozen backbone model f. Pseudo-features for past classes are generated by the following shift:

$$\hat{f}(c_p) = f(c_n) - \mu(c_n) + \mu(c_p) \tag{4}$$

The pseudo-features are then projected into the concept space using the learned concept bottleneck at phase t, W_C^t, to generate pseudo-concepts:

$$\hat{f}_c(c_p) = W_C^t \hat{f}(c_p) \tag{5}$$

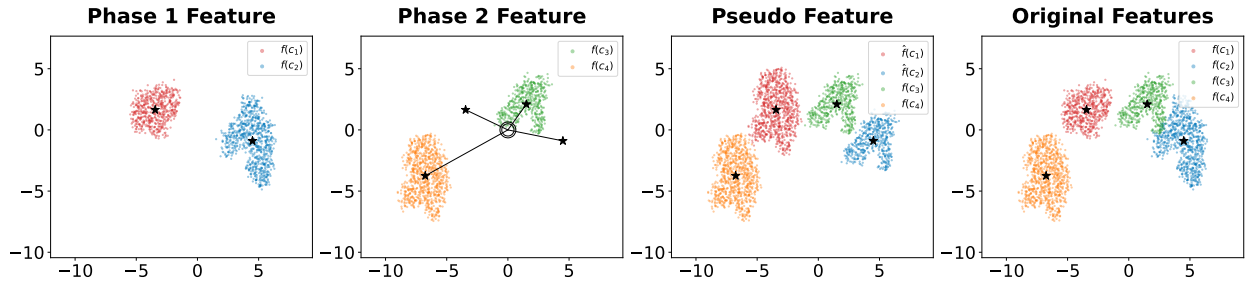

Figure 3: Illustration of the pseudo-feature generation procedure with a toy example. In Phase 1, the model distinguishes between red and blue classes using actual features. In Phase 2, it learns to discriminate among all seen classes (red, blue, orange, green) without access to past-class data. For each past class, the closest new class is identified by cosine similarity between centroids (marked by the $\star$ symbol): orange for red, green for blue. Pseudo-features for past classes are generated by shifting the feature distribution from the closest new class to the target past class. The model then distinguishes all seen classes using actual features for new classes and pseudo-features for past classes. The rightmost subfigure visualizes the actual features for all classes at the end of Phase 2.

These pseudo-concepts for past classes, along with the actual concepts for new classes, are used to train the sparse predictor W_F^t:

$$\min_{W_F^t, b_F^t} \sum_{(x_i,y_i)\in D_1\cup\cdots\cup D_{t-1}} L_{ce}(W_F^t \hat{f}_c(x_i) + b_F^t, y_i) + \sum_{(x_i,y_i)\in D_t} L_{ce}(W_F^t f_c(x_i) + b_F^t, y_i) + \lambda R_\alpha(W_F^t) \tag{6}$$

This allows us to train the model with pseudo-concepts for previous classes, without storing any information except for each class mean.

3.3 Theoretical Perspective

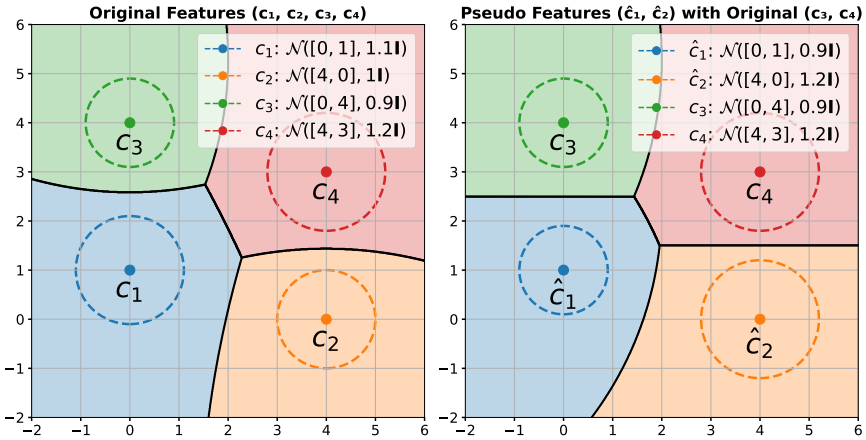

Figure 4: Visualization of decision boundaries in the feature space. Black lines indicate Bayes-optimal boundaries, and colored regions denote predicted class assignments. Dashed circles represent one standard deviation from each class mean. Left: original class feature distributions, where differences in variance lead to curved boundaries between old and new classes. Right: pseudo-feature distributions generated by our method, where matched variances lead to linear boundaries that closely follow the true Bayes decision surfaces.

To further motivate the design of our method, we provide a theoretical analysis based on class distributions in the feature space. Consider a toy example with two learning phases, each introducing two new classes.

We model each class's feature distribution as a multivariate Gaussian $\mathcal{N}(\mu_i, \sigma_i^2 I)$ where $x \in \mathbb{R}^d$. The Bayes optimal decision boundary between classes i and j is where $\log p_i(x) = \log p_j(x)$:

$$\log p_k(x) = -\frac{d}{2}\log(2\pi\sigma_k^2) \; - \; \frac{1}{2\sigma_k^2}\,\|x-\mu_k\|^2,$$

$$\log p_i(x) = \log p_j(x) \iff \frac{1}{\sigma_i^2}\,\|x-\mu_i\|^2 + d\log\sigma_i^2 = \frac{1}{\sigma_j^2}\,\|x-\mu_j\|^2 + d\log\sigma_j^2$$

$$\iff \left(\tfrac{1}{\sigma_j^2} - \tfrac{1}{\sigma_i^2}\right)x^\top x - 2\left(\tfrac{\mu_j}{\sigma_j^2} - \tfrac{\mu_i}{\sigma_i^2}\right)^\top x + \left(\tfrac{\|\mu_j\|^2}{\sigma_j^2} - \tfrac{\|\mu_i\|^2}{\sigma_i^2}\right) = d\,\log\left(\tfrac{\sigma_j^2}{\sigma_i^2}\right).$$

This boundary is generally quadratic but becomes approximately linear when class variances are similar. Our method shifts new class distributions toward old class centroids, forming pseudo-feature distributions with original means and nearby new class variances—e.g., class 1 becomes $\mathcal{N}(\mu_1, \sigma_3^2 I)$, enabling a linear boundary with class 3 due to matched variance. The boundary between real and pseudo-feature distributions closely matches the true boundary, especially when their variances are similar. Figure 4 illustrates this effect. The left panel shows the Bayes-optimal decision regions induced by the original class distributions, where differences in class variances lead to curved boundaries. In contrast, the right panel depicts the pseudo-feature distributions introduced by our method, where the resulting boundaries become linear while still closely approximating the true Bayes decision surfaces. Subsequently, all features (actual features for new classes and pseudo-features for old classes) are projected into the concept space, where concept functionality is preserved via our drift mitigation, enabling concept-based classification.

4 Evaluation

Datasets and Implementation Details. To evaluate the performance of our proposed method, we perform comprehensive experiments on several CIL datasets: CIFAR-10, CIFAR-100 (Krizhevsky et al., 2009), CUB (Wah et al., 2011), TinyImageNet (Le & Yang, 2015), ImageNet-Subset, ImageNet (Deng et al., 2009), and Places365 (Zhou et al., 2017). We employ ResNet-18 (He et al., 2016), DeiT (Touvron et al., 2021), modified to match ResNet-18's parameter count by adjusting the embedding dimension and number of heads, and ViT-Base/16 (Dosovitskiy et al., 2020) as backbone models. The subsequent parameters follow the setup from LF-CBM (Oikarinen et al., 2023). The regularization parameter λ is selected to ensure that each class has 35 to 55 non-zero weights, leading to sparsity levels ranging from 1% to 5% across different datasets. To ensure a fair comparison, we use the same random seed as the compared methods (Zhu et al., 2021b; 2022; Petit et al., 2023; Rymarczyk et al., 2023) to shuffle the classes and split them into phases. Each configuration is evaluated three times, and the average results are reported.

Evaluation Metric. We report the average incremental accuracy as the mean of the average accuracy across all incremental phases, including the first phase. Additionally, we offer average accuracy for each phase to provide an understanding of the accuracy progression throughout the continual learning process. Further, we report the average incremental forgetting in the Appendix.

Comparison to Interpretable Methods. We compare our interpretable model against ICICLE (Rymarczyk et al., 2023) and IN2 (Yang et al., 2024), which, to the best of our knowledge, are the only existing interpretable methods designed for the CIL setting. We also evaluate a full rehearsal strategy, where the training data from all previous phases is stored in memory and accessible for each new phase, though this is highly impractical in real-world settings. However, this approach helps us understand how closely our method reaches the best possible performance. Our backbone model for the CIFAR-10/100, CUB, and Places365 datasets is ResNet-18 pretrained on ImageNet, and for the TinyImageNet and ImageNet datasets, it is pretrained on Places365. For each dataset, we distribute the classes evenly across T phases.

Table 1 (Experiment I) demonstrates that our approach significantly outperforms all the compared interpretable methods. CI-CBM achieves an average improvement of 35.50%, 39.57%, 43.13%, and 26.40% on CIFAR-10, CIFAR-100, CUB[1], and TinyImageNet, respectively. Our performance on the Places365 and

[1]ICICLE used a ResNet-34 backbone pre-trained on ImageNet. We use ResNet-18 for compatibility with most CIL models. With ResNet-34, our results are 62.9, 65.9, and 66.4 for T = 4, 10, and 20 phases, respectively.

Method	CIFAR-10	CIFAR-100			CUB			TinyImageNet			Places365			ImageNet		
	T=5	T=5	T=10	T=20	T=4	T=10	T=20	T=5	T=10	T=20	T=5	T=10	T=20	T=5	T=10	T=20
ICICLE (Rymarczyk et al., 2023)	-	-	-	-	35.0	18.5	9.9	-	-	-	-	-	-	-	-	-
IN2 (Yang et al., 2024)	44.9	41.9	27.5	17.3	30.5	20.1	13.6	30.9	21.4	14.3	-	-	-	-	-	-
CI-CBM (ours)	**80.4**	**68.8**	**68.8**	**67.8**	**62.2**	**65.3**	**66.1**	**48.6**	**48.7**	**48.5**	**48.3**	**49.3**	**49.0**	**31.7**	**32.1**	**31.5**
Full rehearsal	85.9	70.9	72.6	73.4	67.7	67.2	67.1	50.0	51.4	52.5	48.9	50.7	51.6	32.1	33.3	34.1

Table 1: **Experiment I -** Comparisons of the Average Incremental Accuracy of CI-CBM with other interpretable models in CIL. The same pretrained backbone was used to reproduce IN2 (Yang et al., 2024) results for a fair comparison. The results for ICICLE (Rymarczyk et al., 2023) are as reported in their original paper. Cells marked with "-" indicate that results were unavailable. The full rehearsal approach retains all previous training data across phases, providing an upper bound for evaluating CI-CBM's performance.

Method	Interpretability	CIFAR-100			TinyImageNet			ImageNet-Subset		
		T=5	T=10	T=20	T=5	T=10	T=20	T=5	T=10	T=20
EWC† (Kirkpatrick et al., 2017)	✗	24.5	21.2	15.9	18.8	15.8	12.4	-	20.4	-
LWF§ (Li & Hoiem, 2017)	✗	32.4	17.9	14.9	22.3	17.4	12.5	-	23.5	-
iCaRL-CNN§ (Rebuffi et al., 2017)	✗	51.0	48.3	44.6	34.7	31.0	27.8	-	50.5	-
LUCIR† (Hou et al., 2019)	✗	51.2	41.1	25.2	41.7	28.1	18.9	56.8	41.4	28.5
MUC† (Liu et al., 2020)	✗	49.4	30.2	21.3	32.6	26.6	21.9	-	35.1	-
SDC† (Yu et al., 2020)	✗	56.8	57.0	58.9	-	-	-	-	61.2	-
PASS† (Zhu et al., 2021b)	✗	63.5	61.8	58.1	49.6	47.3	42.1	64.4	61.8	51.3
SSRE† (Zhu et al., 2022)	✗	65.9	65.0	61.7	50.4	48.9	48.2	-	67.7	-
FeTrIL† (Petit et al., 2023)	✗	66.3	65.2	61.5	54.8	53.1	52.2	72.2	71.2	67.1
EFC * (Magistri et al., 2024)	✗	-	68.2	65.9	-	57.5	56.5	-	75.4	71.6
SOPE* (Zhu et al., 2023)	✗	66.6	65.8	61.8	53.7	52.9	51.9	-	69.2	-
FCS* (Li et al., 2024)	✗	62.1	60.3	58.3	46.0	44.9	42.5	-	61.7	-
DCMI* (Qiu et al., 2024)	✗	67.9	66.8	64.0	54.8	53.9	52.5	70.5	70.0	65.5
TASS* (Liu et al., 2024)	✗	68.7	67.4	62.7	55.1	54.2	52.7	74.3	72.6	68.7
CI-CBM (ours)	✓	61.9	60.5	60.2	49.2	48.3	47.3	67.6	66.2	62.2
Full rehearsal	✓	63.7	63.5	62.1	50.5	50.4	50.2	71.7	71.7	69.6

Table 2: **Experiment II -** Comparisons of the average incremental accuracy of CI-CBM with EFCIL unrestricted ResNet-based methods across CIFAR-100, TinyImageNet, and ImageNet-Subset in a non-pretrained scenario. Models marked with a † represent reported results from (Petit et al., 2023), while those marked with an § indicate reported findings from (Zhu et al., 2021b), and models marked with a $*$ denote results reported from their paper. Cells marked with "-" indicate that results were unavailable. The full rehearsal approach retains all previous training data across phases, providing an upper bound for evaluating CI-CBM's performance.

ImageNet datasets demonstrates that our proposed approach is capable of incremental classification on challenging large-scale datasets. As the total number of phases increases, our method remains robust and maintains its average incremental accuracy, while the other compared methods fail to do so. By comparing CI-CBM with the impractical full rehearsal scenario, we find that our approach shows only a small 2.6% decrease on average, demonstrating its effectiveness in maintaining learned knowledge without retaining any samples from previous phases.

Comparison to Non-Pretrained and Non-Interpretable Methods. Motivated by the results observed in interpretable models and the investigation of the effect of the pretrained backbone model on our metric scores, we extend our analysis to unrestricted models. We follow FeTrIL (Petit et al., 2023) and APG (Tang et al., 2023) to train ResNet-18 and DeiT, respectively, from scratch in the initial phase. Afterward, we freeze them as the backbone for CI-CBM and incrementally learn the classes. We conduct a comparative analysis of our method against classical approaches (Kirkpatrick et al., 2017; Li & Hoiem, 2017; Rebuffi et al., 2017; Hou et al., 2019), SOTA ResNet-based models (Zhu et al., 2021b;a; 2022; Petit et al., 2023), and SOTA prompt-based methods (Wang et al., 2022c;b; Tang et al., 2023).

In our experiments, we follow the setup described in (Petit et al., 2023; Tang et al., 2023), evaluating CIFAR-100 and ImageNet-Subset under the following configurations: (i) an initial set of 50 classes with 5 phases, each introducing 10 classes, (ii) 50 initial classes followed by 10 phases of 5 classes each, (iii) 40 initial classes

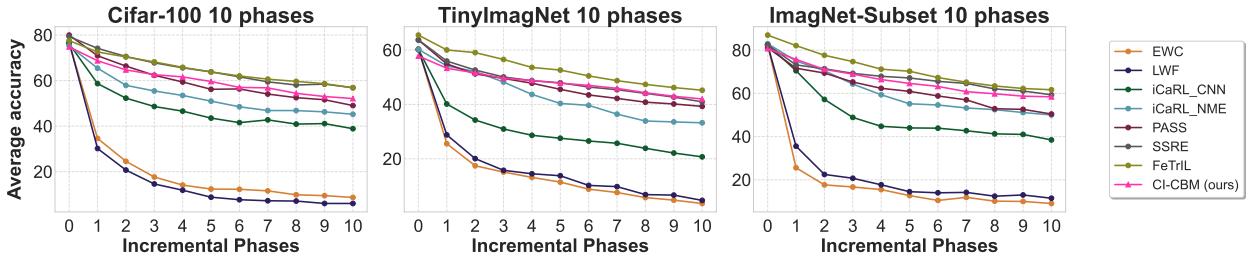

Figure 5: **Experiment III -** Average accuracy curves for CIFAR-100, TinyImageNet, and ImageNet-Subset over 10 learning phases, comparing CI-CBM with other unrestricted ResNet-based methods.

with 20 phases, each introducing 3 classes. Additionally, TinyImageNet is tested with 100 initial classes, with the remaining classes distributed as follows: (i) 5 phases of 20 classes, (ii) 10 phases of 10 classes, (iii) 20 phases of 5 classes.

Table 2 (Experiment II) illustrates that our interpretable model demonstrates superior performance compared to many unrestricted ResNet-based models, with a minimal 7.5% difference in accuracy compared to the SOTA models. Figure 5 (Experiment III) presents the average accuracy curve for CIFAR-100, TinyImageNet, and ImageNet-Subset across 10 phases. Although CI-CBM starts with the lowest accuracy in the initial phase due to interpretability constraints, it effectively learns to distinguish new classes while preserving performance on previously learned classes, ultimately achieving a high average accuracy by the final phase.

Table 3 (Experiment IV) compares the performance of CI-CBM with prompt-based models using a DeiT backbone trained from scratch in the first phase. Without needing any additional prompts, CI-CBM outperforms L2P (Wang et al., 2022c) and DualPrompt (Wang et al., 2022b), two methods that fail to generalize when trained from scratch in the initial phase. CI-CBM achieves performance comparable to APG (Tang et al., 2023), despite the latter's use of prompt generators, which involve cross-attention layers, groups of learnable parameters, and linear layers, leading to a more parameter-intensive model. Results with more incremental phases are reported in the Appendix.

Comparison to Pretrained, Non-Interpretable Methods. Following prior works, we use a ViT-Base/16 model pretrained on ImageNet-21k, utilizing the final [CLS] token as the backbone feature. Table 4 (Experiment V) shows that CI-CBM achieves competitive accuracy, only 7% lower on CIFAR-100 and 3.1% lower on CUB compared to SOTA models, demonstrating that CI-CBM provides interpretability with minimal performance trade-off.

Interpretability and Insights on Model Reasoning. To provide a comprehensive understanding of our model's interpretability, Figure 1 presents a Sankey diagram that offers global insights into the concept-to-class relationships. In the diagram, line widths are proportional to absolute weights, displaying only concepts with absolute weights greater than 0.2. Concepts with negative weights are labeled as "NOT" concepts, and they are organized according to their weight values. The findings reveal that the model consistently relied on

Method	Interpretability	CIFAR-100		ImageNet-Subset	
		T=10	T=20	T=10	T=14
L2P (Wang et al., 2022c)	✗	36.5	18.8	25.1	29.9
DualPrompt (Wang et al., 2022b)	✗	26.8	11.8	35.8	30.3
APG (Tang et al., 2023)	✗	66.6	62.4	75.5	69.8
CI-CBM (ours)	✓	59.5	59.7	54.6	55.6
Full rehearsal	✓	62.7	63.4	58.9	60.4

Table 3: **Experiment IV -** Comparison of the average incremental accuracy between CI-CBM and EFCIL unrestricted prompt-based methods in a non-pretrained scenario. The DeiT backbone model is trained using data from the first phase. Results for the compared methods are reported from (Tang et al., 2023).

Method	Interpretability	CIFAR-100 (T=10)	CUB (T=10)
L2P† (Wang et al., 2022c)	✗	84.6	65.2
DualPrompt† (Wang et al., 2022b)	✗	81.3	68.5
CODA-Prompt† (Smith et al., 2023)	✗	86.3	79.5
APG * (Tang et al., 2023)	✗	89.3	-
LAE *(Gao et al., 2023)	✗	89.9	-
ESN *(Wang et al., 2023)	✗	86.3	-
SimpleCIL† (Zhou et al., 2024a)	✗	87.6	87.1
ConvPrompt * (Roy et al., 2024)	✗	88.8	80.2
EASE† (Zhou et al., 2024c)	✗	87.8	86.8
SAFE† (Zhao et al.)	✗	92.8	91.1
CI-CBM (ours)	✓	85.6	88.0
Full rehearsal	✓	87.8	88.7

Table 4: **Experiment V -**Comparison of average incremental accuracy for CI-CBM and EFCIL unrestricted models with the pretrained ViT-Base/16 backbone. Models marked with a † represent reported results from (Zhao et al.), while models marked with a $*$ denote results reported from their paper. Cells marked with "-" indicate unavailable results.

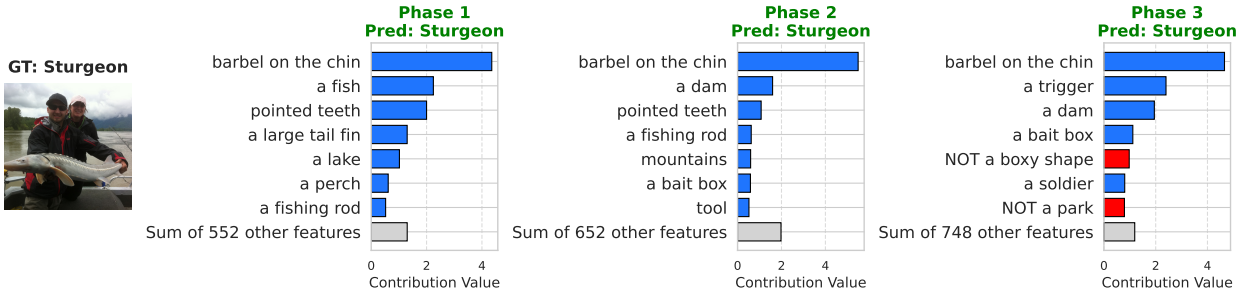

Figure 6: Visualization of model reasoning and concept contributions for an image of the Sturgeon class, introduced in the first phase of the ImageNet-Subset. In the first phase, CI-CBM correctly classifies the image using actual features. In the second and third phases, CI-CBM continues to accurately distinguish it among a larger set of classes by generating pseudo-concepts. Additional visualizations are provided in Supplement Section A12.

the same positive concepts across different phases without needing to impose constraints like freezing weights. Additionally, as new classes were introduced, more discriminative negative concepts were incorporated, enabling the model to better differentiate between similar classes. Furthermore, Figure 6 illustrates the local explanations for individual decisions made by the model using a randomly chosen image from the Sturgeon class in the first phase of the ImageNet-Subset dataset. The contribution of concept j to the output i for input x_k in phase t is given by $\text{Contrib}(x_k, i, j) = W_F^t[i, j] \times f_c^t(x_k)[j]$. This figure effectively demonstrates how the decision layer evolves from relying on actual concepts in the first phase to utilizing pseudo-concepts in subsequent phases. The model continues to classify the image correctly in the later phases, predominantly relying on the correct concepts.

Ablation Study. To assess the effect of each component in CI-CBM, we conduct an ablation study on CIFAR-100 and TinyImageNet datasets, analyzing the average incremental accuracy. Table 5 (Experiment VI) highlights the contributions of concept regularization and pseudo-concept generation. The results are as follows: (i) Skipping pseudo-concept generation leads to weights with zero and negative biases in previous class weights, causing their accuracy to drop to zero and significantly lowering overall performance. (ii) Concept regularization alone cannot prevent this, as it only preserves concepts within the Concept Bottleneck Layer but does not stop the weights for previous classes from being pushed to zero. (iii) Pseudo-concepts improve performance by helping the model distinguish between new and old classes. (iv) Combining pseudo-concept generation with concept regularization provides further performance gains. Furthermore, we discuss the effect of sparsity in the prediction layer and compare our method with IN2 (Yang et al., 2024) in concept set expansion in the Appendix.

Concept reg	Pseudo-Concept	CIFAR-100			TinyImageNet		
		T=5	T=10	T=20	T=5	T=10	T=20
✗	✗	38.0	26.2	16.9	29.1	20.9	14.4
✓	✗	38.0	26.3	16.9	29.2	21.0	14.3
✗	✓	68.4	68.2	67.6	48.2	48.3	48.2
✓	✓	**68.8**	**68.8**	**67.8**	**48.6**	**48.7**	**48.5**

Table 5: **Experiment VI (Ablation Study) -** Performance impact of different components of CI-CBM

5 Conclusion

In this work, we propose **CI-CBM**, an interpretable model for Exemplar-Free Class Incremental Learning (EFCIL). **CI-CBM** extends the Concept Bottleneck Model with concept regularization and pseudo-concept generation to incrementally learn both the concept bottleneck layer and sparse prediction layer. Our approach outperforms other interpretable models designed for EFCIL, achieving an average accuracy gain of 36% and approaching SOTA black-box model performance, demonstrating effectiveness in both pretrained and non-pretrained settings. We further illustrate how **CI-CBM**'s decision-making adapts with new phases, providing insights at both global and local levels, and present ablation studies to assess the impact of various components of our model.

References

Rahaf Aljundi, Francesca Babiloni, Mohamed Elhoseiny, Marcus Rohrbach, and Tinne Tuytelaars. Memory aware synapses: Learning what (not) to forget. In *Proceedings of the European conference on computer vision (ECCV)*, pp. 139–154, 2018.

Jihwan Bang, Heesu Kim, YoungJoon Yoo, Jung-Woo Ha, and Jonghyun Choi. Rainbow memory: Continual learning with a memory of diverse samples. In *Proceedings of the IEEE/CVF conference on computer vision and pattern recognition*, pp. 8218–8227, 2021.

Eden Belouadah and Adrian Popescu. Deesil: Deep-shallow incremental learning. In *Proceedings of the European Conference on Computer Vision (ECCV) Workshops*, pp. 0–0, 2018.

Mariusz Bojarski. End to end learning for self-driving cars. *arXiv preprint arXiv:1604.07316*, 2016.

Pietro Buzzega, Matteo Boschini, Angelo Porrello, Davide Abati, and Simone Calderara. Dark experience for general continual learning: a strong, simple baseline. *Advances in neural information processing systems*, 33:15920–15930, 2020.

Arslan Chaudhry, Marc'Aurelio Ranzato, Marcus Rohrbach, and Mohamed Elhoseiny. Efficient lifelong learning with a-gem. *arXiv preprint arXiv:1812.00420*, 2018.

Matthias De Lange, Rahaf Aljundi, Marc Masana, Sarah Parisot, Xu Jia, Aleš Leonardis, Gregory Slabaugh, and Tinne Tuytelaars. A continual learning survey: Defying forgetting in classification tasks. *IEEE transactions on pattern analysis and machine intelligence*, 44(7):3366–3385, 2021.

Jia Deng, Wei Dong, Richard Socher, Li-Jia Li, Kai Li, and Li Fei-Fei. Imagenet: A large-scale hierarchical image database. In *2009 IEEE conference on computer vision and pattern recognition*, pp. 248–255. Ieee, 2009.

Prithviraj Dhar, Rajat Vikram Singh, Kuan-Chuan Peng, Ziyan Wu, and Rama Chellappa. Learning without memorizing. In *Proceedings of the IEEE/CVF conference on computer vision and pattern recognition*, pp. 5138–5146, 2019.

Alexey Dosovitskiy, Lucas Beyer, Alexander Kolesnikov, Dirk Weissenborn, Xiaohua Zhai, Thomas Unterthiner, Mostafa Dehghani, Matthias Minderer, Georg Heigold, Sylvain Gelly, et al. An image is worth 16x16 words: Transformers for image recognition at scale. *arXiv preprint arXiv:2010.11929*, 2020.

Arthur Douillard, Matthieu Cord, Charles Ollion, Thomas Robert, and Eduardo Valle. Podnet: Pooled outputs distillation for small-tasks incremental learning. In *Computer vision–ECCV 2020: 16th European conference, Glasgow, UK, August 23–28, 2020, proceedings, part XX 16*, pp. 86–102. Springer, 2020.

Qiankun Gao, Chen Zhao, Yifan Sun, Teng Xi, Gang Zhang, Bernard Ghanem, and Jian Zhang. A unified continual learning framework with general parameter-efficient tuning. In *Proceedings of the IEEE/CVF International Conference on Computer Vision*, pp. 11483–11493, 2023.

Rui Gao and Weiwei Liu. Ddgr: Continual learning with deep diffusion-based generative replay. In *International Conference on Machine Learning*, pp. 10744–10763. PMLR, 2023.

Ian J Goodfellow, Mehdi Mirza, Da Xiao, Aaron Courville, and Yoshua Bengio. An empirical investigation of catastrophic forgetting in gradient-based neural networks. *arXiv preprint arXiv:1312.6211*, 2013.

Filip Guzy, Michał Woźniak, and Bartosz Krawczyk. Evaluating and explaining generative adversarial networks for continual learning under concept drift. In *2021 International Conference on Data Mining Workshops (ICDMW)*, pp. 295–303. IEEE, 2021.

Tyler L Hayes and Christopher Kanan. Lifelong machine learning with deep streaming linear discriminant analysis. In *Proceedings of the IEEE/CVF conference on computer vision and pattern recognition workshops*, pp. 220–221, 2020.

Kaiming He, Xiangyu Zhang, Shaoqing Ren, and Jian Sun. Deep residual learning for image recognition. In *Proceedings of the IEEE conference on computer vision and pattern recognition*, pp. 770–778, 2016.

Geoffrey Hinton. Distilling the knowledge in a neural network. *arXiv preprint arXiv:1503.02531*, 2015.

Saihui Hou, Xinyu Pan, Chen Change Loy, Zilei Wang, and Dahua Lin. Learning a unified classifier incrementally via rebalancing. In *Proceedings of the IEEE/CVF conference on computer vision and pattern recognition*, pp. 831–839, 2019.

Aya Abdelsalam Ismail, Julius Adebayo, Hector Corrada Bravo, Stephen Ra, and Kyunghyun Cho. Concept bottleneck generative models. In *The Twelfth International Conference on Learning Representations*, 2023.

James Kirkpatrick, Razvan Pascanu, Neil Rabinowitz, Joel Veness, Guillaume Desjardins, Andrei A Rusu, Kieran Milan, John Quan, Tiago Ramalho, Agnieszka Grabska-Barwinska, et al. Overcoming catastrophic forgetting in neural networks. *Proceedings of the national academy of sciences*, 114(13):3521–3526, 2017.

Pang Wei Koh, Thao Nguyen, Yew Siang Tang, Stephen Mussmann, Emma Pierson, Been Kim, and Percy Liang. Concept bottleneck models. In *International conference on machine learning*, pp. 5338–5348. PMLR, 2020.

Alex Krizhevsky, Geoffrey Hinton, et al. Learning multiple layers of features from tiny images. 2009.

Akshay Kulkarni, Ge Yan, Chung-En Sun, Tuomas Oikarinen, and Tsui-Wei Weng. Interpretable generative models through post-hoc concept bottlenecks. In *IEEE/CVF Conference on Computer Vision and Pattern Recognition*, 2025.

Ya Le and Xuan Yang. Tiny imagenet visual recognition challenge. *CS 231N*, 7(7):3, 2015.

Qiwei Li, Yuxin Peng, and Jiahuan Zhou. Fcs: Feature calibration and separation for non-exemplar class incremental learning. In *Proceedings of the IEEE/CVF conference on computer vision and pattern recognition*, pp. 28495–28504, 2024.

Zhizhong Li and Derek Hoiem. Learning without forgetting. *IEEE transactions on pattern analysis and machine intelligence*, 40(12):2935–2947, 2017.

Xialei Liu, Jiang-Tian Zhai, Andrew D Bagdanov, Ke Li, and Ming-Ming Cheng. Task-adaptive saliency guidance for exemplar-free class incremental learning. In *Proceedings of the IEEE/CVF Conference on Computer Vision and Pattern Recognition*, pp. 23954–23963, 2024.

Yu Liu, Sarah Parisot, Gregory Slabaugh, Xu Jia, Ales Leonardis, and Tinne Tuytelaars. More classifiers, less forgetting: A generic multi-classifier paradigm for incremental learning. In *Computer Vision–ECCV 2020: 16th European Conference, Glasgow, UK, August 23–28, 2020, Proceedings, Part XXVI 16*, pp. 699–716. Springer, 2020.

David Lopez-Paz and Marc'Aurelio Ranzato. Gradient episodic memory for continual learning. *Advances in neural information processing systems*, 30, 2017.

Simone Magistri, Tomaso Trinci, Albin Soutif-Cormerais, Joost van de Weijer, and Andrew D Bagdanov. Elastic feature consolidation for cold start exemplar-free incremental learning. *arXiv preprint arXiv:2402.03917*, 2024.

Michael McCloskey and Neal J Cohen. Catastrophic interference in connectionist networks: The sequential learning problem. In *Psychology of learning and motivation*, volume 24, pp. 109–165. Elsevier, 1989.

Volodymyr Mnih. Playing atari with deep reinforcement learning. *arXiv preprint arXiv:1312.5602*, 2013.

Tuomas Oikarinen and Tsui-Wei Weng. Clip-dissect: Automatic description of neuron representations in deep vision networks. *International Conference on Learning Representations*, 2023.

Tuomas Oikarinen, Subhro Das, Lam M. Nguyen, and Tsui-Wei Weng. Label-free concept bottleneck models. In *International Conference on Learning Representations (ICLR)*, 2023.

Aristeidis Panos, Yuriko Kobe, Daniel Olmeda Reino, Rahaf Aljundi, and Richard E Turner. First session adaptation: A strong replay-free baseline for class-incremental learning. In *Proceedings of the IEEE/CVF International Conference on Computer Vision*, pp. 18820–18830, 2023.

German I Parisi, Ronald Kemker, Jose L Part, Christopher Kanan, and Stefan Wermter. Continual lifelong learning with neural networks: A review. *Neural networks*, 113:54–71, 2019.

Arijit Patra and J Alison Noble. Incremental learning of fetal heart anatomies using interpretable saliency maps. In *Medical Image Understanding and Analysis: 23rd Conference, MIUA 2019, Liverpool, UK, July 24–26, 2019, Proceedings 23*, pp. 129–141. Springer, 2020.

Grégoire Petit, Adrian Popescu, Hugo Schindler, David Picard, and Bertrand Delezoide. Fetril: Feature translation for exemplar-free class-incremental learning. In *Proceedings of the IEEE/CVF winter conference on applications of computer vision*, pp. 3911–3920, 2023.

Ameya Prabhu, Philip HS Torr, and Puneet K Dokania. Gdumb: A simple approach that questions our progress in continual learning. In *Computer Vision–ECCV 2020: 16th European Conference, Glasgow, UK, August 23–28, 2020, Proceedings, Part II 16*, pp. 524–540. Springer, 2020.

Zihuan Qiu, Yi Xu, Fanman Meng, Hongliang Li, Linfeng Xu, and Qingbo Wu. Dual-consistency model inversion for non-exemplar class incremental learning. In *2024 IEEE/CVF Conference on Computer Vision and Pattern Recognition (CVPR)*, pp. 24025–24035. IEEE Computer Society, 2024.

Alec Radford, Jong Wook Kim, Chris Hallacy, Aditya Ramesh, Gabriel Goh, Sandhini Agarwal, Girish Sastry, Amanda Askell, Pamela Mishkin, Jack Clark, et al. Learning transferable visual models from natural language supervision. In *International conference on machine learning*, pp. 8748–8763. PMLR, 2021.

Sylvestre-Alvise Rebuffi, Alexander Kolesnikov, Georg Sperl, and Christoph H Lampert. icarl: Incremental classifier and representation learning. In *Proceedings of the IEEE conference on Computer Vision and Pattern Recognition*, pp. 2001–2010, 2017.

Olaf Ronneberger, Philipp Fischer, and Thomas Brox. U-net: Convolutional networks for biomedical image segmentation. In *Medical image computing and computer-assisted intervention–MICCAI 2015: 18th international conference, Munich, Germany, October 5-9, 2015, proceedings, part III 18*, pp. 234–241. Springer, 2015.

Anurag Roy, Riddhiman Moulick, Vinay K Verma, Saptarshi Ghosh, and Abir Das. Convolutional prompting meets language models for continual learning. In *Proceedings of the IEEE/CVF Conference on Computer Vision and Pattern Recognition*, pp. 23616–23626, 2024.

Cynthia Rudin. Stop explaining black box machine learning models for high stakes decisions and use interpretable models instead. *Nature machine intelligence*, 1(5):206–215, 2019.

Andrei A Rusu, Neil C Rabinowitz, Guillaume Desjardins, Hubert Soyer, James Kirkpatrick, Koray Kavukcuoglu, Razvan Pascanu, and Raia Hadsell. Progressive neural networks. *arXiv preprint arXiv:1606.04671*, 2016.

Dawid Rymarczyk, Joost van de Weijer, Bartosz Zieliński, and Bartlomiej Twardowski. Icicle: Interpretable class incremental continual learning. In *Proceedings of the IEEE/CVF International Conference on Computer Vision*, pp. 1887–1898, 2023.

James Seale Smith, Leonid Karlinsky, Vyshnavi Gutta, Paola Cascante-Bonilla, Donghyun Kim, Assaf Arbelle, Rameswar Panda, Rogerio Feris, and Zsolt Kira. Coda-prompt: Continual decomposed attention-based prompting for rehearsal-free continual learning. In *Proceedings of the IEEE/CVF conference on computer vision and pattern recognition*, pp. 11909–11919, 2023.

Robert Speer and Catherine Havasi. Conceptnet 5: A large semantic network for relational knowledge. *The People's Web Meets NLP: Collaboratively Constructed Language Resources*, pp. 161–176, 2013.

Chung-En Sun, Tuomas Oikarinen, Berk Ustun, and Tsui-Wei Weng. Concept bottleneck large language models. *ICLR*, 2025.

Yu-Ming Tang, Yi-Xing Peng, and Wei-Shi Zheng. When prompt-based incremental learning does not meet strong pretraining. In *Proceedings of the IEEE/CVF International Conference on Computer Vision*, pp. 1706–1716, 2023.

Hoang Thanh-Tung and Truyen Tran. Catastrophic forgetting and mode collapse in gans. In *2020 international joint conference on neural networks (ijcnn)*, pp. 1–10. IEEE, 2020.

Hugo Touvron, Matthieu Cord, Matthijs Douze, Francisco Massa, Alexandre Sablayrolles, and Hervé Jégou. Training data-efficient image transformers & distillation through attention. In *International conference on machine learning*, pp. 10347–10357. PMLR, 2021.

Gido M Van de Ven and Andreas S Tolias. Three scenarios for continual learning. *arXiv preprint arXiv:1904.07734*, 2019.

Catherine Wah, Steve Branson, Peter Welinder, Pietro Perona, and Serge Belongie. The caltech-ucsd birds-200-2011 dataset. 2011.

Shipeng Wang, Xiaorong Li, Jian Sun, and Zongben Xu. Training networks in null space of feature covariance for continual learning. In *Proceedings of the IEEE/CVF conference on Computer Vision and Pattern Recognition*, pp. 184–193, 2021.

Yabin Wang, Zhiwu Huang, and Xiaopeng Hong. S-prompts learning with pre-trained transformers: An occam's razor for domain incremental learning. *Advances in Neural Information Processing Systems*, 35: 5682–5695, 2022a.

Yabin Wang, Zhiheng Ma, Zhiwu Huang, Yaowei Wang, Zhou Su, and Xiaopeng Hong. Isolation and impartial aggregation: A paradigm of incremental learning without interference. In *Proceedings of the AAAI Conference on Artificial Intelligence*, volume 37, pp. 10209–10217, 2023.

Zifeng Wang, Zizhao Zhang, Sayna Ebrahimi, Ruoxi Sun, Han Zhang, Chen-Yu Lee, Xiaoqi Ren, Guolong Su, Vincent Perot, Jennifer Dy, et al. Dualprompt: Complementary prompting for rehearsal-free continual learning. In *European conference on computer vision*, pp. 631–648. Springer, 2022b.

Zifeng Wang, Zizhao Zhang, Chen-Yu Lee, Han Zhang, Ruoxi Sun, Xiaoqi Ren, Guolong Su, Vincent Perot, Jennifer Dy, and Tomas Pfister. Learning to prompt for continual learning. In *Proceedings of the IEEE/CVF conference on computer vision and pattern recognition*, pp. 139–149, 2022c.

Eric Wong, Shibani Santurkar, and Aleksander Madry. Leveraging sparse linear layers for debuggable deep networks. In *International Conference on Machine Learning*, pp. 11205–11216. PMLR, 2021.

Chenshen Wu, Luis Herranz, Xialei Liu, Joost Van De Weijer, Bogdan Raducanu, et al. Memory replay gans: Learning to generate new categories without forgetting. *Advances in neural information processing systems*, 31, 2018.

Yue Wu, Yinpeng Chen, Lijuan Wang, Yuancheng Ye, Zicheng Liu, Yandong Guo, and Yun Fu. Large scale incremental learning. In *Proceedings of the IEEE/CVF conference on computer vision and pattern recognition*, pp. 374–382, 2019.

Shipeng Yan, Jiangwei Xie, and Xuming He. Der: Dynamically expandable representation for class incremental learning. In *Proceedings of the IEEE/CVF conference on computer vision and pattern recognition*, pp. 3014–3023, 2021.

Sin-Han Yang, Tuomas Oikarinen, and Tsui-Wei Weng. Concept-driven continual learning. *Transactions on Machine Learning Research*, 2024. ISSN 2835-8856. URL `https://openreview.net/forum?id=HSW49uvCNW`.

Jaehong Yoon, Eunho Yang, Jeongtae Lee, and Sung Ju Hwang. Lifelong learning with dynamically expandable networks. *arXiv preprint arXiv:1708.01547*, 2017.

Lu Yu, Bartlomiej Twardowski, Xialei Liu, Luis Herranz, Kai Wang, Yongmei Cheng, Shangling Jui, and Joost van de Weijer. Semantic drift compensation for class-incremental learning. in 2020 ieee. In *CVF Conference on Computer Vision and Pattern Recognition (CVPR)*, pp. 6980–6989, 2020.

Mert Yuksekgonul, Maggie Wang, and James Zou. Post-hoc concept bottleneck models. *arXiv preprint arXiv:2205.15480*, 2022.

Xiaohua Zhai, Basil Mustafa, Alexander Kolesnikov, and Lucas Beyer. Sigmoid loss for language image pre-training. In *Proceedings of the IEEE/CVF International Conference on Computer Vision*, pp. 11975–11986, 2023.

Li Zhang, Youwei Liang, Ruiyi Zhang, Amirhosein Javadi, and Pengtao Xie. Blo-sam: Bi-level optimization based finetuning of the segment anything model for overfitting-preventing semantic segmentation. In *Forty-first International Conference on Machine Learning*, 2024.

Yuheng Zhang, Ruoxi Jia, Hengzhi Pei, Wenxiao Wang, Bo Li, and Dawn Song. The secret revealer: Generative model-inversion attacks against deep neural networks. In *Proceedings of the IEEE/CVF conference on computer vision and pattern recognition*, pp. 253–261, 2020.

Linglan Zhao, Xuerui Zhang, Ke Yan, Shouhong Ding, and Weiran Huang. Safe: Slow and fast parameter-efficient tuning for continual learning with pre-trained models, 2024. *URL https://arxiv.org/abs/2411.02175*.

Bolei Zhou, Agata Lapedriza, Aditya Khosla, Aude Oliva, and Antonio Torralba. Places: A 10 million image database for scene recognition. *IEEE transactions on pattern analysis and machine intelligence*, 40(6): 1452–1464, 2017.

Da-Wei Zhou, Zi-Wen Cai, Han-Jia Ye, De-Chuan Zhan, and Ziwei Liu. Revisiting class-incremental learning with pre-trained models: Generalizability and adaptivity are all you need. *International Journal of Computer Vision*, pp. 1–21, 2024a.

Da-Wei Zhou, Hai-Long Sun, Jingyi Ning, Han-Jia Ye, and De-Chuan Zhan. Continual learning with pre-trained models: A survey. *arXiv preprint arXiv:2401.16386*, 2024b.

Da-Wei Zhou, Hai-Long Sun, Han-Jia Ye, and De-Chuan Zhan. Expandable subspace ensemble for pre-trained model-based class-incremental learning. In *Proceedings of the IEEE/CVF Conference on Computer Vision and Pattern Recognition*, pp. 23554–23564, 2024c.

Fei Zhu, Zhen Cheng, Xu-Yao Zhang, and Cheng-lin Liu. Class-incremental learning via dual augmentation. *Advances in Neural Information Processing Systems*, 34:14306–14318, 2021a.

Fei Zhu, Xu-Yao Zhang, Chuang Wang, Fei Yin, and Cheng-Lin Liu. Prototype augmentation and self-supervision for incremental learning. In *Proceedings of the IEEE/CVF Conference on Computer Vision and Pattern Recognition*, pp. 5871–5880, 2021b.

Kai Zhu, Wei Zhai, Yang Cao, Jiebo Luo, and Zheng-Jun Zha. Self-sustaining representation expansion for non-exemplar class-incremental learning. In *Proceedings of the IEEE/CVF Conference on Computer Vision and Pattern Recognition*, pp. 9296–9305, 2022.

Kai Zhu, Kecheng Zheng, Ruili Feng, Deli Zhao, Yang Cao, and Zheng-Jun Zha. Self-organizing pathway expansion for non-exemplar class-incremental learning. In *Proceedings of the IEEE/CVF International Conference on Computer Vision*, pp. 19204–19213, 2023.

A1 Appendix Overview

In this section, we provide a brief overview of the Appendix contents. The Appendix is primarily focused on (i) defining precise evaluation metrics for the CIL setting, (ii) presenting extended experiments and ablation studies that analyze the behavior of CI-CBM across different backbones and regimes, and (iii) showcasing additional qualitative visualizations that illustrate model reasoning and weight structure.

First, in Section A2, we discuss the main limitations of our method. Section A3 defines the metrics used throughout our CIL evaluations and reports extended results on average incremental forgetting across three backbones and datasets (Experiments VII–IX). Sections A4–A8 present a series of ablation studies examining concept generation, sparsity, concept-set size, robustness to noisy concept activations, and an alternative strategy for learning the prediction layer (Experiments X–XIV). In Section A9, we analyze our unique-concept expansion mechanism and its effect on model size and interpretability (Experiment XVI). Section A10 evaluates the challenging one-class-increment regime (Experiment XV). Section A11 details the full concept-generation pipeline, including prompts, few-shot examples, and filtering steps. Finally, Section A12 provides additional qualitative visualizations of model weights and per-image concept attributions that complement the figures in the main paper.

A2 Limitation

The main limitations of our research point to future directions. First, the model sometimes forms incorrect correlations between specific concepts and classes, warranting further investigation to see if this stems from the training process or vision-language model misalignments. Second, our pseudo-concept generation relies on basic geometric translations and projections. A more refined approach to generating realistic pseudo-concepts could reduce overlap between old and new classes, improving model performance.

A3 Metrics for the CIL Setting and Further Experiments

Let $a_{i,j}$ denote the model's accuracy on the j-th task after learning the i-th task, where $i \geqslant j$. The following standard metrics are used to evaluate continual learning performance, assuming each phase contains an equal amount of data:

- Average Phase Accuracy:

$$A_t = \frac{1}{t} \sum_{j=1}^{t} a_{t,j} \tag{A1}$$

- Average Phase Forgetting:

$$F_t = \frac{1}{t-1} \sum_{j=1}^{t-1} \max_{i \in \{1,\ldots,t-1\}} (a_{i,j} - a_{t,j}) \tag{A2}$$

- Average Incremental Accuracy:

$$\bar{A} = \frac{1}{T} \sum_{t=1}^{T} A_t \tag{A3}$$

- Average Incremental Forgetting:

$$\bar{F} = \frac{1}{T-1} \sum_{t=2}^{T} F_t \tag{A4}$$

For scenarios with unbalanced phases, such as when the first phase contains a larger number of classes for backbone pretraining, a weighted version of average phase accuracy and forgetting should be calculated, where the weights are proportional to the size of each phase.

Method	CIFAR-100				TinyImageNet				ImageNet-Subset			
	T=5	T=10	T=20	T=60	T=5	T=10	T=20	T=100	T=5	T=10	T=20	T=60
CI-CBM	11.4	13.0	17.1	19.3	8.4	9.5	10.9	14.6	11.9	13.6	16.9	19.5
Full rehearsal	8.8	8.7	11.0	11.7	7.0	7.2	7.4	7.8	7.0	7.1	8.1	8.6

Table A1: **Experiment VII -** Average incremental forgetting of CI-CBM in the non-pretrained scenario with the ResNet-18 backbone, trained on first-phase data from CIFAR-100, TinyImageNet, and ImageNet-Subset, and evaluated under 5, 10, 20, and 60 incremental phase settings. The full rehearsal approach retains all previous training data across phases, providing an upper bound for evaluating CI-CBM's performance. (Complementary to the results in Table 2).

Method	T	CIFAR-100		ImageNet-Subset	
		$\bar{A}$	$\bar{F}$	$\bar{A}$	$\bar{F}$
CI-CBM (ours)	5	60.1	8.5	56.2	6.6
	10	59.5	8.5	54.6	8.9
	20	59.7	10.2	54.4	10.8
	60	58.5	11.7	52.3	13.4
Full rehearsal	5	62.5	4.4	58.6	4.1
	10	62.7	4.5	58.9	4.6
	20	63.4	5.1	59.6	5.5
	60	63.4	6.0	59.0	6.4

Table A2: **Experiment VIII -** Average incremental accuracy ($\bar{A}$) and forgetting ($\bar{F}$) of CI-CBM in the non-pretrained scenario with the DeiT backbone, trained on first-phase data from CIFAR-100 and ImageNet-Subset, and evaluated under 5, 10, 20, and 60 incremental phase settings. The full rehearsal approach retains all previous training data across phases, providing an upper bound for evaluating CI-CBM's performance. (Complementary to Table 3).

Method	T	CIFAR-100		CUB	
		$\bar{A}$	$\bar{F}$	$\bar{A}$	$\bar{F}$
CI-CBM (ours)	5	85.6	6.5	87.6	4.9
	10	85.6	7.9	88.0	4.5
	20	85.3	9.0	88.2	4.6
Full rehearsal	5	87.0	3.3	88.5	4.0
	10	87.8	3.4	88.7	3.5
	20	88.2	3.8	88.7	4.2

Table A3: **Experiment IX -** Average incremental accuracy ($\bar{A}$) and forgetting ($\bar{F}$) of CI-CBM in the pretrained scenario with the ImageNet-pretrained ViT-B/16 backbone, evaluated under 5, 10, and 20 incremental phase settings. The full rehearsal approach retains all previous training data across phases, providing an upper bound for evaluating CI-CBM's performance. (Complementary to Table 4).

Tables A1 (Experiment VII) and A2 (Experiment VIII) present the average incremental forgetting in the non-pretrained scenario with the ResNet-18 and DeiT backbones, respectively. Table A3 (Experiment IX) presents the average incremental forgetting in the pretrained scenario with the ViT-B/16-IN21K backbone.

A4 Alternative Concept Generation Methods

We conduct an experiment to evaluate the importance of using GPT-3 for our model's performance by comparing it against generating the initial concept sets with ConceptNet (Speer & Havasi, 2013). Note that ConceptNet is not a language model but rather a knowledge graph. The results in Table A4 (Experiment X) show that our proposed pipeline, when using the concept sets generated from ConceptNet, still performs well on CIFAR-100 and TinyImageNet. However, there is a slight decrease in accuracy (approximately a 2% drop) compared to using GPT-3-generated concepts. Furthermore, we observe that ConceptNet completely fails on CUB, whereas GPT-3-generated concepts achieve strong results. This highlights the effectiveness of GPT-3 in generating concepts for fine-grained datasets where ConceptNet struggles.

A5 Impact of Sparsity on Model Performance

Table A5 (Experiment XI) presents the effect of sparsity along with the corresponding sparsity levels. Wong et al. (2021) proposed fitting a sparse linear prediction layer on top of deep feature representations, showing

Method	CIFAR-100			CUB			TinyImageNet		
	T=5	T=10	T=20	T=5	T=10	T=20	T=5	T=10	T=20
CI-CBM (ConceptNet)	66.8	67.1	66.5	27.6	24.3	23.8	48.3	48.4	47.8
CI-CBM (GPT-3 [original])	**68.8**	**68.8**	**67.8**	**62.2**	**65.3**	**66.1**	**48.6**	**48.7**	**48.5**

Table A4: **Experiment X (Ablation Study) -** ConceptNet vs. GPT-3 for initial concept set generation

Method	CIFAR-100			TinyImageNet		
	T=5	T=10	T=20	T=5	T=10	T=20
CI-CBM (dense)	68.4	68.6	**68.3**	46.5	47.0	47.0
CI-CBM (sparse [original])	**68.8**	**68.8**	67.8	**48.6**	**48.7**	**48.5**
Sparsity	4.84%	5.70%	7.02%	2.06%	2.43%	3.36%

Table A5: **Experiment XI (Ablation Study) -** Performance impact of sparsity constraints

that sparse models are more interpretable while maintaining high accuracy. Our results generally suggest that removing the sparsity constraint neither improves performance nor interpretability. During training, our goal is to optimize the prediction layer to distinguish between pseudo-concepts of past classes and actual concepts of new classes, expecting that the learned layer will classify both old and new classes based on their actual concepts in the test datasets. A dense layer might overly focus on the pseudo-concept distribution, while a sparse prediction layer relies on fewer concepts per class, making it more robust and yielding slightly better performance.

A6 Effect of Concept Set Size on Performance

Table A6 (Experiment XII) presents the impact of reducing the number of available concepts during training. We simulate reduced concept availability by randomly masking a portion of the concept set and training the model using only the remaining subset. This setting evaluates the model's robustness to incomplete or noisy concept supervision. As shown, performance remains relatively stable even when only 25% of the concept set is used, with less than a 3.5% drop in accuracy for CIFAR-100 and a 2.1% drop for TinyImageNet.

	CIFAR-100				TinyImageNet			
Concept Use	100%	75%	50%	25%	100%	75%	50%	25%
Accuracy	68.8	68.4	67.5	65.5	48.6	48.0	47.5	46.5

Table A6: **Experiment XII (Ablation Study) -** Accuracy vs. concept availability.

A7 Robustness to Noise in Image-Concept Alignment

To evaluate the sensitivity of our method to noise in concept supervision, we inject Gaussian noise into the concept activation matrix P at different signal-to-noise ratio (SNR) levels during training. Table A7 (Experiment XIII) reports accuracy for SNR levels of 10 dB, 5 dB, and 0 dB. We observe that performance degrades only marginally as noise increases, indicating that the model remains robust even under noisy concept activations.

A8 Alternative Approach for Learning the Prediction Layer

In addition to our proposed approach, we evaluate an alternative method for learning the prediction layer.

	CIFAR-100				TinyImageNet			
SNR Level	None	10 dB	5 dB	0 dB	None	10 dB	5 dB	0 dB
Accuracy (%)	68.8	68.6	68.1	67.9	48.6	48.3	48.2	47.4

Table A7: **Experiment XIII (Ablation Study) -** Accuracy vs. SNR in image-concept alignment.

We expand the prediction layer for new classes when a new phase arrives, while freezing the weights for previously learned classes. The focus is on discriminating between new classes and preventing loss of class separability across phases. As shown in Table A8 (Experiment XIV), while this approach performs well for $T = 5$, where each phase introduces enough classes to reduce overlap, the performance drops significantly for $T = 20$, as fewer new classes are introduced per phase, leading to greater overlap. In contrast, CI-CBM focuses on maintaining global separability by generating pseudo-concepts, resulting in robust performance across different values of T.

Method	CIFAR-100			TinyImageNet		
	T=5	T=10	T=20	T=5	T=10	T=20
Local Class Discrimination	63.5	55.2	42.6	46.4	41.3	33.2
CI-CBM	**68.8**	**68.8**	**67.8**	**48.6**	**48.7**	**48.5**

Table A8: **Experiment XIV (Ablation Study) -** Performance comparison of alternative prediction layer learning strategy.

Method	Interpretability	CIFAR-100 (T=60)	TinyImageNet (T=100)	ImageNet-Subset (T=60)
FeTrIL (Petit et al., 2023)	✗	59.8	50.2	65.4
DSLDA (Hayes & Kanan, 2020)	✗	60.5	52.6	63.6
CI-CBM (ours)	✓	55.9	44.8	60.8
Full rehearsal	✓	62.0	50.1	69.3

Table A9: **Experiment XV -** Comparison of the average incremental accuracy of CI-CBM and FeTrIL (Petit et al., 2023) and DSLDA (Hayes & Kanan, 2020) in a setting where each incremental phase introduces one new class. This setting represents a special case of Table 1.

A9 Unique Concept Expansion

Our approach also ensures that only unique concepts are added during each new phase of learning. When a new phase arrives, concepts for the newly introduced classes are generated using GPT-3. However, due to possible similarities between some new concepts and existing classes, naively adding all generated concepts to the concept set can lead to multiple versions of the same concept in the set. Unlike IN2 (Yang et al., 2024), which incorporates duplicate concepts, we ensure that only truly new concepts are added to prevent this redundancy. Figure A1 (Experiment XVI) illustrates the difference in the number of concepts per seen class when duplication is avoided (Unique Concept Set Expansion) versus when all generated concepts are added (Cumulative Concept Count). As shown, avoiding duplication results in nearly half the number of concepts by the final phase. This leads to a much lighter concept bottleneck layer and prediction layer, enabling more efficient optimization and significantly improving interpretability.

A10 One-Class Increments in EFCIL

Table A9 (Experiment XV) presents results for one-class increments, a task that many EFCIL methods struggle with, as they typically require at least two classes per increment to effectively update the model. The table reports results for CIFAR-100 and ImageNet-Subset with an initial phase of 40 classes and 60 incremental phases, and for TinyImageNet with an initial phase of 100 classes and 100 incremental phases.

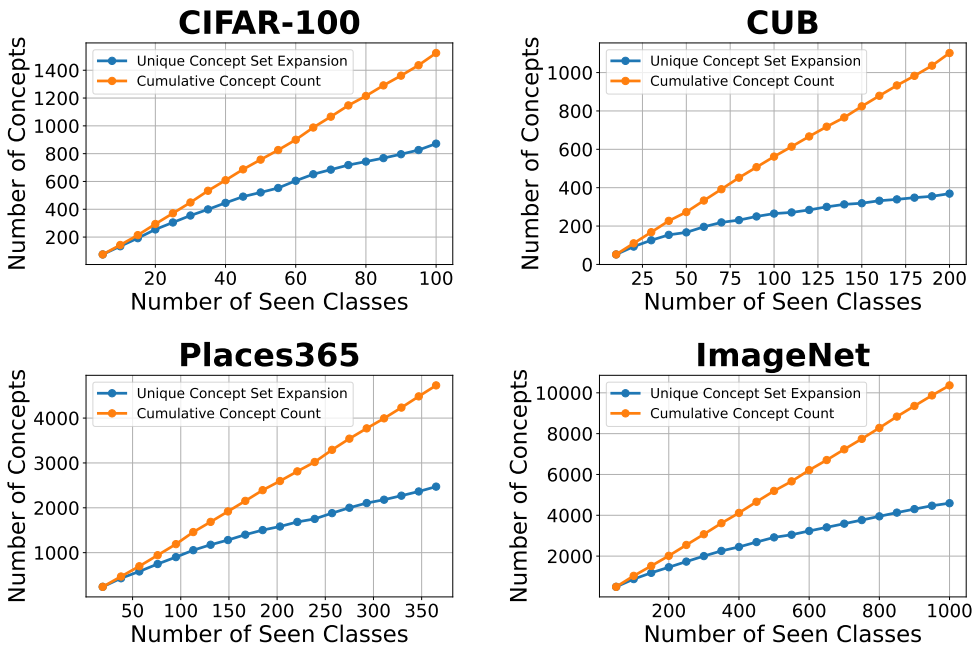

Figure A1: **Experiment XVI (Ablation Study) -** Comparison of the number of concepts used per number of seen classes across different datasets for $T = 20$ phases.

A11 Concept Generation Pipeline

For each new class, we generate candidate concepts using a fixed set of language prompts to query GPT-3. Following the design of LF-CBM (Oikarinen et al., 2023), we apply the following three prompts:

- "List the most important features for recognizing something as a {class}."
- "List the things most commonly seen around a {class}."
- "Give superclasses for the word {class}."

Each prompt is issued twice to increase diversity, and responses are combined to form an initial concept pool. To improve consistency, we use few-shot prompting with two fixed example classes and their expected outputs. These examples are shared across all datasets and phases.

The raw concept set is then filtered in three stages:

1. Length filter: Remove concepts longer than 30 characters.
2. Class similarity filter: Remove concepts with cosine similarity > 0.85 to any class name, using Sentence-Transformer and CLIP text embeddings.
3. Redundancy filter: Remove near-duplicate concepts with cosine similarity > 0.9 to any earlier concept in the set.

This filtered set is then used to update the concept set. All steps are automated and applied incrementally for each new phase. The full pipeline is implemented in the released codebase.

A12 Additional Visualization for Model Reasoning

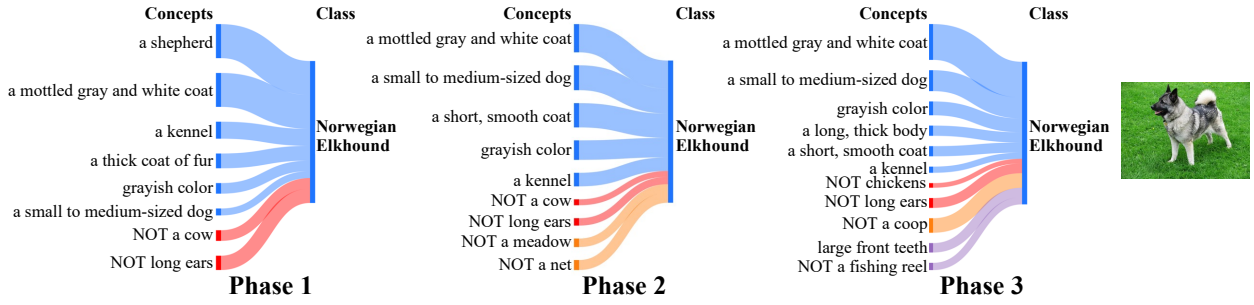

Figure A2: Visualization of the final layer weights with absolute values greater than 0.2 for the **Norwegian Elkhound** class in the ImageNet-Subset dataset under a five-phase scenario. Concepts with negative weights are labeled as "NOT" concepts. Positive and negative concepts in phase 1 are shown in blue and red, respectively, while concepts added in phases 2 and 3 are shown in orange and purple. The thickness of each edge corresponds to the absolute value of the weight. (Complementary to Figure 1)

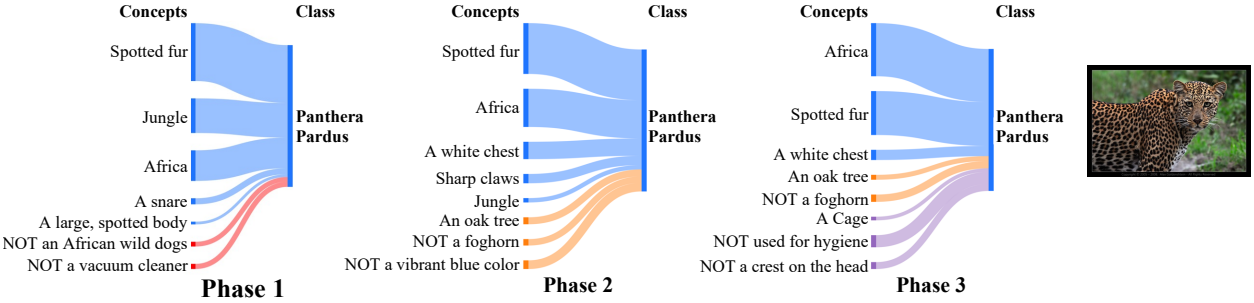

Figure A3: Visualization of the final layer weights with absolute values greater than 0.2 for the **Panthera Pardus** class in the ImageNet-Subset dataset under a five-phase scenario. Concepts with negative weights are labeled as "NOT" concepts. Positive and negative concepts in phase 1 are shown in blue and red, respectively, while concepts added in phases 2 and 3 are shown in orange and purple. The thickness of each edge corresponds to the absolute value of the weight. (Complementary to Figure 1)

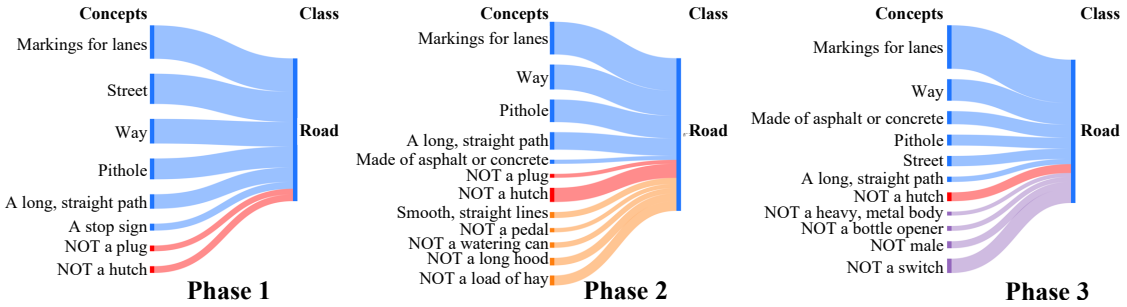

Figure A4: Visualization of the final layer weights with absolute values greater than 0.2 for the **Road** class in the CIFAR-100 dataset under a five-phase scenario. Concepts with negative weights are labeled as "NOT" concepts. Positive and negative concepts in phase 1 are shown in blue and red, respectively, while concepts added in phases 2 and 3 are shown in orange and purple. The thickness of each edge corresponds to the absolute value of the weight. (Complementary to Figure 1)

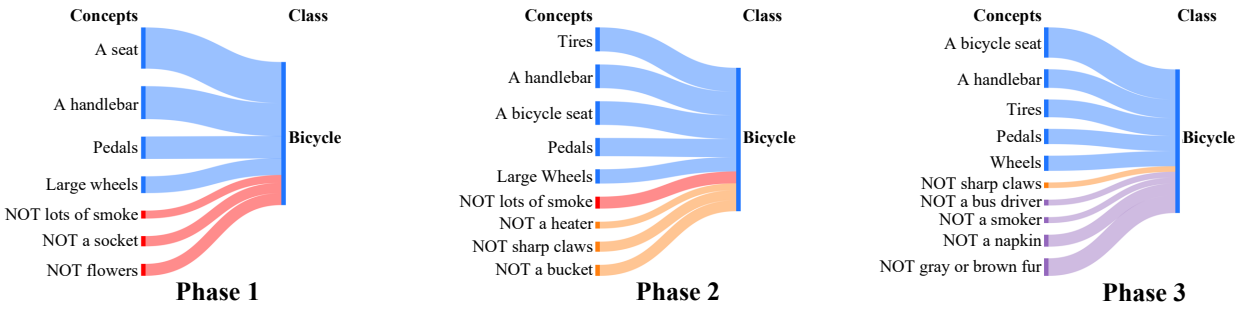

Figure A5: Visualization of the final layer weights with absolute values greater than 0.2 for the **Bicycle** class in the CIFAR-100 dataset under a five-phase scenario. Concepts with negative weights are labeled as "NOT" concepts. Positive and negative concepts in phase 1 are shown in blue and red, respectively, while concepts added in phases 2 and 3 are shown in orange and purple. The thickness of each edge corresponds to the absolute value of the weight. (Complementary to Figure 1)

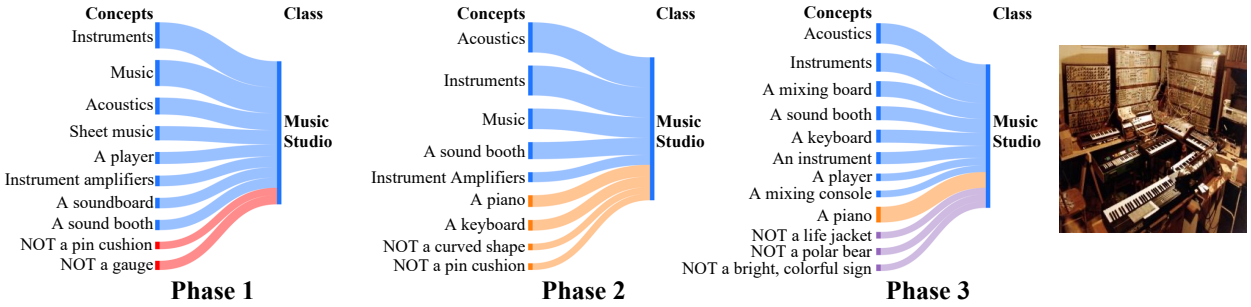

Figure A6: Visualization of the final layer weights with absolute values greater than 0.2 for the **Music Studio** class in the Places365 dataset under a five-phase scenario. Concepts with negative weights are labeled as "NOT" concepts. Positive and negative concepts in phase 1 are shown in blue and red, respectively, while concepts added in phases 2 and 3 are shown in orange and purple. The thickness of each edge corresponds to the absolute value of the weight. (Complementary to Figure 1)

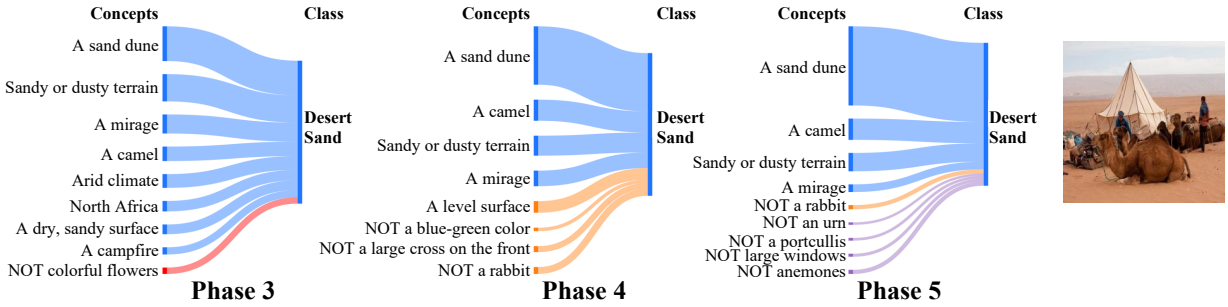

Figure A7: Visualization of the final layer weights with absolute values greater than 0.2 for the **Desert (Sand)** class in the Places365 dataset under a five-phase scenario. Concepts with negative weights are labeled as "NOT" concepts. Positive and negative concepts in phase 3 are shown in blue and red, respectively, while concepts added in phases 4 and 5 are shown in orange and purple. The thickness of each edge corresponds to the absolute value of the weight. (Complementary to Figure 1)

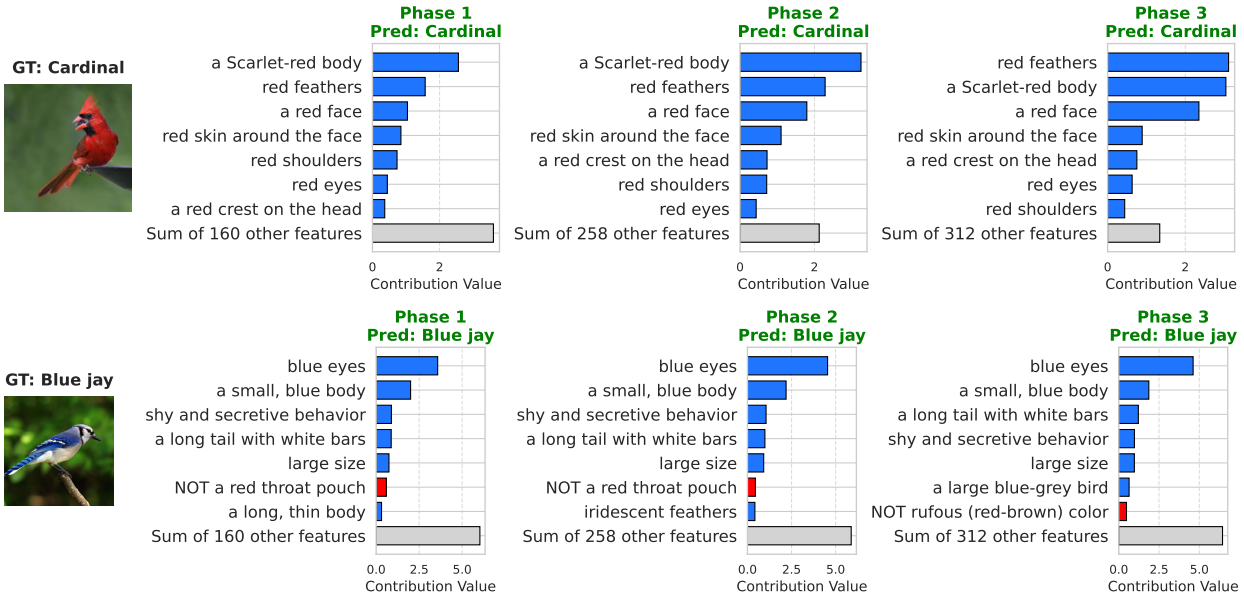

Figure A8: Visualization of model reasoning and concept contributions for images of the Cardinal and Blue Jay classes, introduced in the first phase of the CUB dataset. (Complementary to Figure 6)

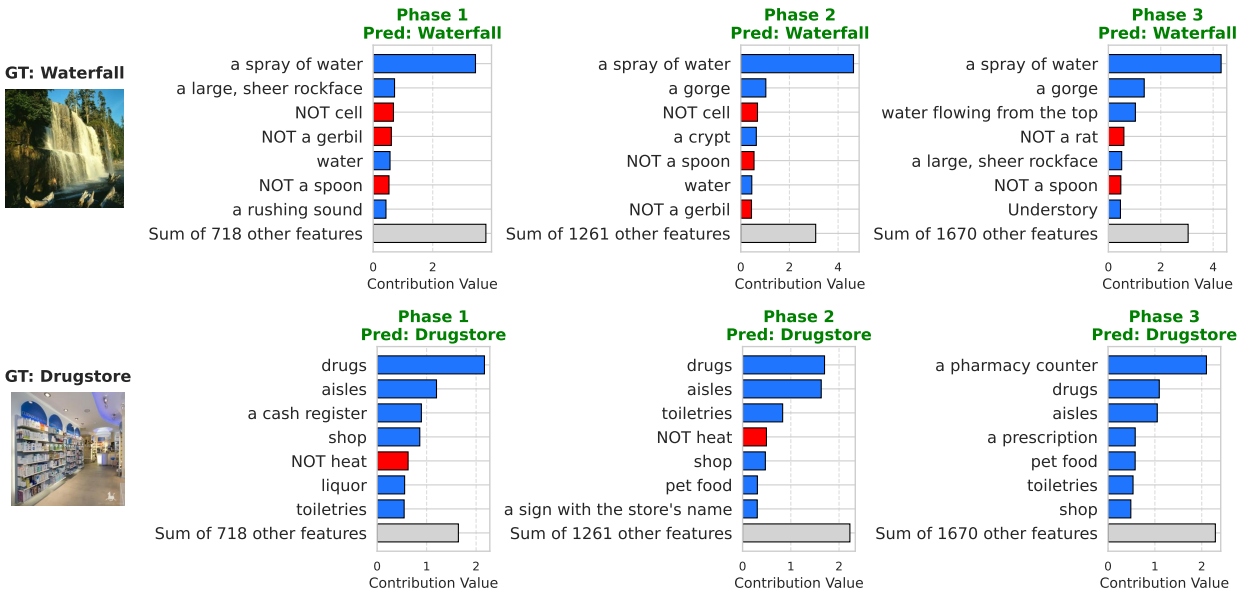

Figure A9: Visualization of model reasoning and concept contributions for images of the Waterfall and Drugstore classes, introduced in the first phase of the Places365 dataset. (Complementary to Figure 6)

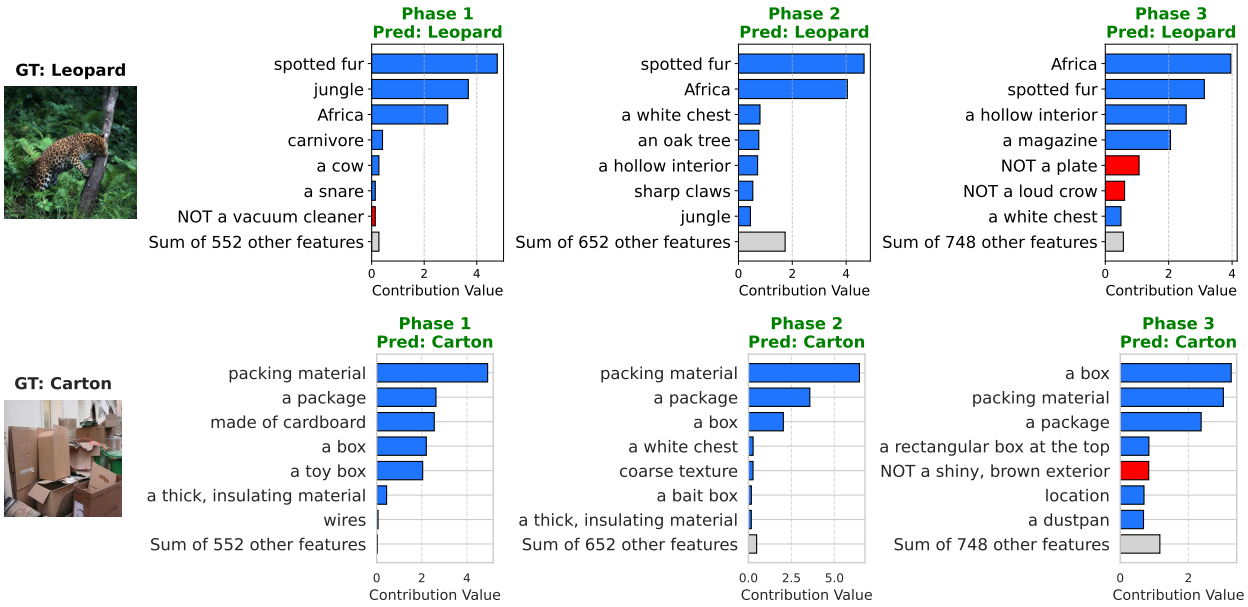

Figure A10: Visualization of model reasoning and concept contributions for images of the Leopard and Carton classes, introduced in the first phase of the ImageNet-Subset. (Complementary to Figure 6)